Mechanistic and functional aspects of the Ruminococcin C sactipeptide isoforms

Lama Shamseddine, Clarisse Roblin, Iris Veyrier, Christian Basset, Lisa de Macedo, Anne Boyeldieu, Marc Maresca, Cendrine Nicoletti, Gaël Brasseur, Sylvie Kieffer– Jaquinod, et al.

iScience

CellPress
OPEN ACCESS

Article

Mechanistic and functional aspects of the Ruminococcin C sactipeptide isoforms

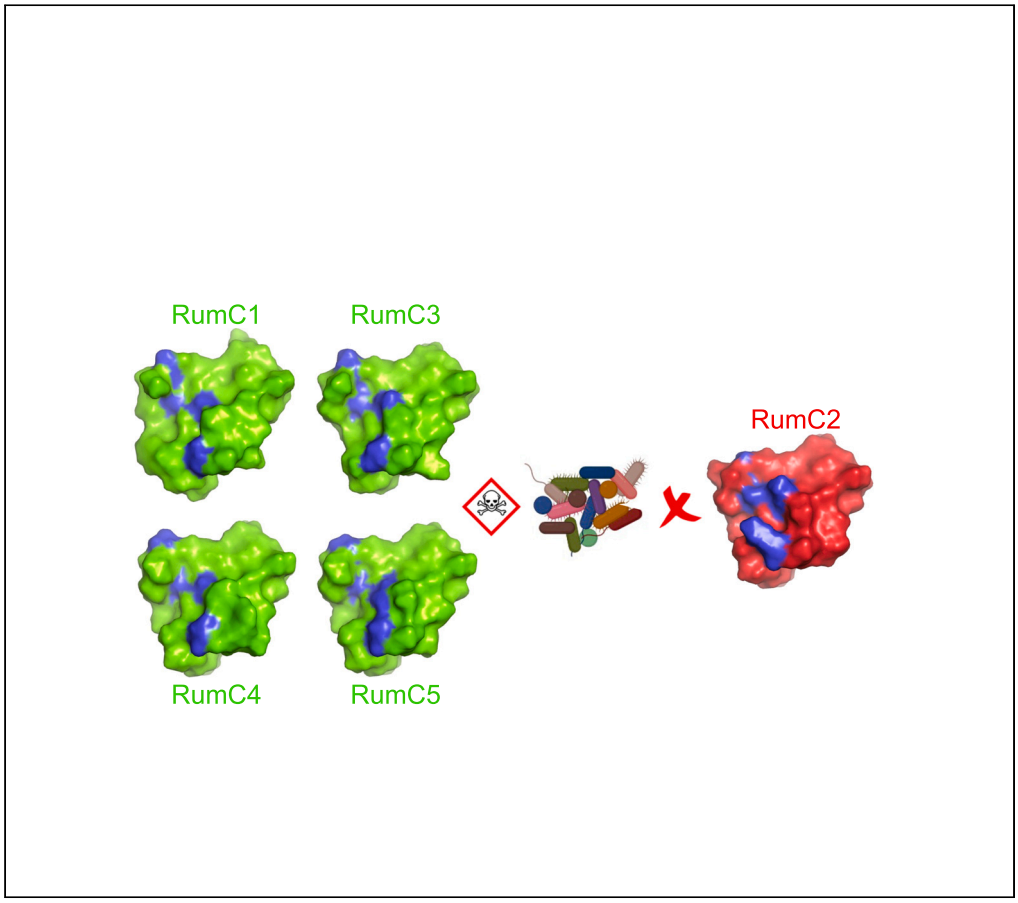

Lama Shamseddine, Clarisse Roblin, Iris Veyrier, ..., Josette Perrier, Victor Duarte, Mickael Lafond

victor.duarte@cea.fr (V.D.)
michael.lafond@univ-amu.fr (M.L.)

Highlights

Reports the structural and functional characterizations of five RumC isoforms

Reveals unexpected variation in antibacterial efficacy between isoforms

Sheds light on key residues essential for antibacterial activity

Identifies synergistic actions of RumC1 in combination with conventional antibiotics

Shamseddine et al., iScience 26, 107563
September 15, 2023
https://doi.org/10.1016/j.isci.2023.107563

iScience

CellPress
OPEN ACCESS

Article

Mechanistic and functional aspects of the Ruminococcin C sactipeptide isoforms

Lama Shamseddine,[1,2,7] Clarisse Roblin,[2,7] Iris Veyrier,[2] Christian Basset,[1] Lisa De Macedo,[1] Anne Boyeldieu,[3] Marc Maresca,[2] Cendrine Nicoletti,[2] Gaël Brasseur,[4] Sylvie Kieffer-Jaquinod,[5] Élise Courvoisier-Dezord,[2] Agnès Amouric,[2] Philippe Carpentier,[1] Nathalie Campo,[3] Mathieu Bergé,[3] Patrice Polard,[3] Josette Perrier,[2] Victor Duarte,[1,*] and Mickael Lafond[2,6,8,*]

SUMMARY

In a scenario where the discovery of new molecules to fight antibiotic resistance is a public health concern, ribosomally synthesized and post-translationally modified peptides constitute a promising alternative. In this context, the Gram-positive human gut symbiont *Ruminococcus gnavus* E1 produces five sactipeptides, Ruminococcins C1 to C5 (RumC1–C5), co-expressed with two radical SAM maturases. RumC1 has been shown to be effective against various multidrug resistant Gram-positives clinical isolates. Here, after adapting the biosynthesis protocol to obtain the four mature RumC2-5 we then evaluate their antibacterial activities. Establishing first that both maturases exhibit substrate tolerance, we then observed a variation in the antibacterial efficacy between the five isoforms. We established that all RumCs are safe for humans with interesting multifunctionalities. While no synergies where observed for the five RumCs, we found a synergistic action with conventional antibiotics targeting the cell wall. Finally, we identified crucial residues for antibacterial activity of RumC isoforms.

INTRODUCTION

Ribosomally synthesized and post-translationally modified peptides (RiPPs) are being considered as potential alternatives to conventional antibiotics in the concerning current context of infectious disease resurgence, associated with increasing antibiotic resistance and a lack of new antimicrobials.[1] RiPPs biosynthesis involves 3 main steps: (1) a ribosomal synthesis of a precursor peptide composed of at least a leader and a core sequence; (2) the introduction of post-translational modification(s) on the core sequence by one or several maturation enzymes; and (3) the export of the modified core peptide combined with the release by specific proteolysis of the leader peptide, resulting in a free form of the active peptide into the extracellular compartment.[2]

Among these RiPPs, sactipeptides form a small but growing subfamily currently comprising 11 characterized members.[3,4] Sactipeptides are featured by one or several sulfur-to-alpha carbon thioether cross-links introduced by radical SAM enzymes and can be further divided into three subfamilies (Figures 1A and 1C).[4,5] The first and oldest subclass (Type I) comprises subtilosin A,[6] thurincin H,[7] the sporulation killing factor (SkfA),[8] thuricin CD[9] that consists of two peptides, Trn-α and Trn-β, thuricin Z also named huazacin,[10,11] and hyicin 4244[12] (Figures 1B and 1C). This type I subclass is characterized by cysteine enriched sequences in the N-terminal part while the amino acid partners of the sactionine linkages are located in the C-terminal part, thus folding the core peptide in a single hairpin shape (Figures 1B and 1C). So far, the identified members of this subclass are mainly produced by *Bacillus* spp. as well as *Staphylococcus hyicus* and display a mostly hydrophobic surface associated with a pore-forming antibacterial mode of action. Recently, we discovered a new sactipeptide — concomitantly confirmed by Balty et al., (2019) — from the human gut symbiont *Ruminococcus gnavus* E1 and demonstrated that Ruminococcin C (RumC) constitutes a second subclass (Type II) of sactipeptides.[13–15] Indeed, due to the presence of cysteine residues in both N- and C-terminal halves of the peptide, the four sactionine bridges fold the peptide in a double hairpin shape (Figures 1B–1D). Since then, streptosactin and QmpA, respectively produced by the oral commensal *Streptococcus thermophilus* and the porcine pathogen *Streptococcus suis*, have been identified with a similar distribution of cysteine residues and folding, expanding this second sactipeptide group[16,17] (Figure 1C). Finally, a third subclass (Type III) of sactipeptides has emerged very recently with the

[1]University Grenoble Alpes, CNRS UMR5249, CEA, IRIG, Laboratoire Chimie et Biologie des Métaux, 38054 Grenoble, France
[2]Aix Marseille University, CNRS, Centrale Marseille, iSm2, 13013 Marseille, France
[3]Laboratoire de Microbiologie et Génétique Moléculaires (LMGM), Centre de Biologie Intégrative (CBI), Toulouse, France
[4]Laboratoire de Chimie Bactérienne, CNRS-Université Aix-Marseille UMR, Institut de Microbiologie de la Méditerranée, Marseille, France
[5]Université Grenoble Alpes, CEA, INSERM, IRIG, Biologie à Grande Echelle (BGE), 38054 Grenoble, France
[6]INRAE, Aix-Marseille University, UMR1163 Biodiversité et Biotechnologie Fongiques, 13009 Marseille, France
[7]These authors contributed equally
[8]Lead contact
*Correspondence: victor.duarte@cea.fr (V.D.), michael.lafond@univ-amu.fr (M.L.)
https://doi.org/10.1016/j.isci.2023.107563

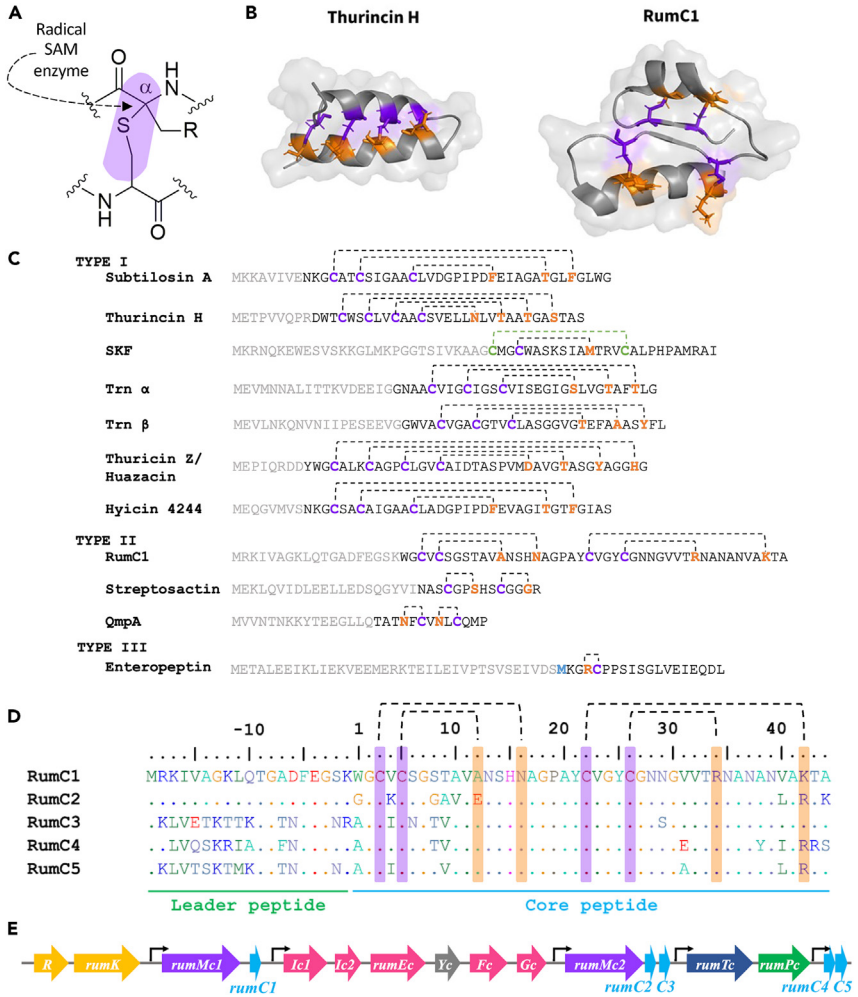

Figure 1. Sactipeptides and RumCs

(A) Sactionine linkage or sulfur-to-α-carbon thioether bond catalyzed by radical SAM enzymes. (B-D) Purple indicates cysteine residues, orange highlights the residues partners of the sacti-bridges, sactionine linkages are shown in black dashed lines whereas disulfide connections are shown in green, and N-methylornithine residue is shown in blue.

(B) Examples of type I and type II sactipeptides associated with a simple hairpin (Thurincin H, PDB: 2LBZ) or a double hairpin (RumC1, PDB: 6T33) structures.

(C) Sequences of identified type I, II and III sactipeptides. Gray indicates the leader sequence.

(D) Peptide sequence of the precursors (leader + core peptide) and the mature (core peptide) isoforms of RumC.

(E) Biosynthetic gene cluster of RumC. Yellow, purple, light blue, pink, dark blue, green and gray indicate genes involve in regulation, maturation, precursor synthesis, immunity, transport, proteolysis and unknown function, respectively.

identification of enteropeptins from *Enterococcus cecorum* which carry an unusual *N*-methylornithine residue in addition to a sactionine bridge[4] (Figure 1C).

RumC is naturally produced in the form of 5 isoforms (RumC1-5).[14,18] The percentage of identity between these isoforms is comprised between 72 and 82% when considering the precursor peptides, and 75–86% when considering the core peptides only (Figure 1D). The production of these isoforms relies on the expression of a biosynthetic gene cluster comprising five genes encoding precursor peptides (i.e., *rumC1* to *rumC5*), two genes encoding sactisynthases (i.e., *rumMc1* and *rumMc2*), as well as genes presumed to be involved in the regulation, immunity and export[14,18] (Figure 1E). Previously, we were able to isolate the 5 isoforms of RumC from cecal contents of *R. gnavus* E1 mono-colonized rats.[14] The mass spectrometry fingerprint of their post-translational modifications revealed that they all displayed 4 sactionine linkages involving the four conserved cysteines and amino acid partners located at the same positions. Moreover, we were able to produce a mature RumC1 by heterologous co-expression of *rumC1*, *rumMc1* and *suf* machinery in *Escherichia coli*. We further characterized the maturation of RumC1 and demonstrated that the leader sequence of the precursor peptide is necessary for the maturation enzyme (RumMc1) to perform the sactionine linkages on the core sequence.[15] In addition, we have shown that the RumC1 active form is obtained *in vivo* after a two-step proteolysis involving first an intracellular pre-cleavage of the leader peptide by RumPc, and then a subsequent cleavage in the luminal

Table 1. Antibacterial activity of the different isoforms of RumC on Gram-positive bacteria

Organism	Strain number	MIC RumC1 (μM)	MIC RumC2 (μM)	MIC RumC3 (μM)	MIC RumC4 (μM)	MIC RumC5 (μM)
Clostridium perfringens	ATCC 13124	0.8	R	2.6	8.3	0.8
Clostridium difficile	DSMZ 1296	0.6	R	25	8.3	2.1
Listeria monocytogenes	DSM 20600	0.8	R	3.1	0.8	6.2
Bacillus cereus	CIP 5257	1.6	R	29.1	6.25	1.3
Bacillus subtilis	ATCC 6633	0.1	R	1.3	0.3	0.1
Streptococcus pneumoniae	R 1501	0.8	R	3.1	1.6	0.7
Vancomycin-resistant *Enterococcus faecalis*	DSMZ 13591	3.1	R	16.6	25	6.2
Methicillin-resistant *Staphylococcus aureus*	ATCC BAA-1717	10.4	R	50	66.6	12.5

Activity spectra of RumC1-5 against Gram-positive. Bacteria were considered resistant (R) when the MICs were greater than 100 μM. MICs were determined in independent triplicates.

compartment by the human pancreatic trypsin.[14] Thanks to a biomimetic production route, we obtained a sufficient amount of RumC1 to solve its 3D-structure and study its biological roles.[15,19] Unlike the first subclass of sactipeptides, RumC1 exhibits a mostly hydrophilic surface that is associated with a non-pore-forming antibacterial mechanism of action targeting Gram positive pathogens. We showed the undeniable therapeutic interest of RumC1 based on its activity *in vivo* on an infected animal model as well as *ex vivo* in a complex gut microbiome environment; its host beneficial activities such as a positive influence on gut homeostasis, an anti-inflammatory activity and a wound healing effect; and finally its drug-like features namely safety for human tissues, stability and undetectable propensity for spontaneous resistance selection.[19]

This extensive work on RumC1 raised several key interlinked questions on the four other RumCs isoforms, mainly on their maturation by either RumMc1 or RumMc2 and their biological functions. In addition, the structure-function relationships that dictate the antimicrobial activity of the RumC isoforms were still unexplored. Finally, a potential synergetic antibacterial effect between these isoforms or in combination with conventional antibiotics remained an untested and promising avenue. In this study we therefore decided to explore these different aspects, to go further in the knowledge of this subclass of sactipeptide.

RESULTS

Heterologous production of mature RumC2-5 isoforms

We previously reported that the thioether network, clearly characterized in RumC1, is conserved in the four other isoforms RumC2-5 produced *in vivo* by *R. gnavus* E1.[14] Here we first sought to determine whether the two sactisynthases are able to modify the five RumC peptides adapting the maturation scheme that we previously established for RumC1 by RumMc1 in *E. coli*.[14] Thus, we attempted to produce the mature form of each RumC isoform following their heterologous co-expression as precursor peptides with either RumMc1 or RumMc2 and in presence of the *suf* machinery.[14,15] The three-step purification protocol involves a dextrin affinity column, a size exclusion chromatography, and finally a C18 reverse phase HPLC to separate the leader sequence from the mature core peptide after trypsin digestion. Except for the RumMc2/RumC2 pair, all the other combinations allowed us to produce the fully mature form of the RumC isoforms corresponding to the mature peptides previously isolated from mono-associated rat model. As expected, LC-MS/MS analyses confirmed that RumC2-5 mature peptides contain four thioether bridges involving residues at the same positions as those identified in RumC1 (Figure S1). Since our goal was to perform biological assays, we selected the sactisynthase/substrate combination that allowed us to isolate each mature RumC isoform with the highest yield and degree of purity. Under our heterologous production conditions, the best results were obtained with the RumMc1 sactisynthase regardless of the RumC sequences. Figure S2 shows the reverse phase chromatogram profiles and the purity analysis by SDS-PAGE obtained for the selected pairs. The observed production yields are in the range of 1 mg/L culture for RumC1, RumC3, and RumC5 and 0.3 mg/L for RumC2 and RumC4. As revealed by the HPLC profiles, the mature form of each RumC isoform was obtained together with truncated sequences that originate from trypsin cleavage of the leader peptide and the unmodified core peptide. Indeed, as reported previously for RumC1, the unmodified core peptide is subject to trypsin cleavage at positions 34 and 42 (Figure 1D), whereas these amino acid residues are protected if they are involved in the thioether linkages.[14,15]

RumC isoforms share the same antibacterial spectra with different potencies

The antibacterial spectra of RumC1-5 were investigated on a broad range of Gram-positive and negative bacteria, including pathogens and antibiotic-resistant strains (Tables 1 and 2). Out of the 5 isoforms, 4 displayed antibacterial activity against the same species with variation in the degree of efficacy. Surprisingly, RumC2 showed no antibacterial activity on the 13 strains included in this trial. Among the active isoforms, we found that RumC1 and RumC5 are the most potent with similar MICs on almost all strains, lower or in the micromolar range for *Clostridium perfringens, Clostridium difficile, Listeria monocytogenes* (for RumC1 only), *Bacillus cereus, Bacillus subtilis,* and *Streptococcus pneumoniae*

Table 2. Antibacterial activity of the different isoforms of RumC on Gram-negative bacteria

Organism	Strain number	MIC RumC1 (μM)	MIC RumC2 (μM)	MIC RumC3 (μM)	MIC RumC4 (μM)	MIC RumC5 (μM)
Vibrio alginolyticus	DSM 2172	0.06	R	0.6	0.1	0.05
Helicobacter pylori	ATCC 43504	12.5	R	100	100	25
Escherichia coli	ATCC 8739	R	R	R	R	R
Pseudomonas aeruginosa	ATCC 9027	R	R	R	R	R
Acinetobacter baumanii	CIP 110431	R	R	R	R	R
Δ Escherichia coli (imp4213)	CIP 111272	18.7	75	30.3	20.8	16.7

Activity spectra of RumC1-5 against Gram-negative. Bacteria were considered resistant (R) when the MICs were greater than 100 μM. MICs were determined in independent triplicates.

(Table 1). RumC3 and RumC4 showed higher MICs values, although RumC4 displays MIC values similar to RumC1 and RumC5 on *L. monocytogenes, B. subtilis*, and *S. pneumoniae*. Unexpectedly, we observed that all the active RumC isoforms - i.e., except RumC2 - are able to inhibit the growth of *Vibrio alginolyticus* and *Helicobacter pylori* whereas it has been shown that RumC1 was only active against Gram-positive bacteria.[14,15,19] In particular, the four isoforms are very efficient against *V. alginolyticus* with MICs under the micromolar ranges. Since it has been established that *H. pylori* and *V. alginolyticus* express LPS whose composition differs from that of other Gram-negative bacteria[20,21] we hypothesized that the lack of activity toward other Gram-negative bacteria could arise from the LPS acting as a barrier. To strengthen this hypothesis, we assayed the activity of RumC isoforms on an *E. coli* K-12 strain carrying the *imp4213* mutation causing a deletion on the LptD protein involved in LPS transport and leading to increase outer membrane permeability.[22] Interestingly, all isoforms, including RumC2, displayed activity against this strain with MICs ranging from 16.7 to 75 μM, even if RumC2 is the less active of the five RumCs (Table 2) Thus, it seems that RumC1, 3, 4, 5 are inactive against most of Gram-negative bacteria not because their molecular target is specific to Gram-positive bacteria, but rather due to the fact they are unable to cross the outer membrane layer of Gram-negative bacteria. As for RumC2, its inactivity on the Gram-positive and Gram-negative bacteria assayed in this study could be related to its sequence divergence with the four other RumCs, where one or more amino acids would be crucial for the activity or for the intake through the cell membrane. Finally, RumC1 remains globally the most efficient isoform.

RumC isoforms display a similar mode of action

We previously showed that RumC1 has a non-pore forming antibacterial mechanism of action involving depletion of intracellular ATP contents in *C. perfringens*.[14,15] Since we observed variations in the degree of efficacy of the different isoforms, we checked whether they could be related to different modes of action. As RumC2 is not active against the bacterial pathogenic strains assayed, we only compared RumC1, 3, 4 and 5. To assess the permeabilization potency of the different isoforms, we followed the incorporation of propidium iodide into *C. perfringens*, a fluorescent DNA intercalating agent unable to cross undamaged cellular membranes. Cetyltrimethylammonium bromide (CTAB) and the pore forming RiPP nisin were used as positive controls of permeabilization. After 10 min treatment, permeabilization with nisin already resulted in 45% of the maximum PI incorporation measured with CTAB and increased up to ~70% within 1 h. Conversely, with all the active antibacterial RumC isoforms, less than 3.5% of permeabilization was measured after 10 min exposure at 5xMIC. Permeabilization increased up to ~20% after 1 h of treatment for all isoforms, indicating that the primary mechanism of action of RumC isoforms is not a pore-forming action but eventually leads to partial cell lysis, a possible consequence of cell death (Figure 2A). To confirm that the antibacterial activity of RumC indirectly and ultimately leads to cell lysis, we observed cell permeabilization in the presence of RumC. For practical reasons and because the isoforms seem to follow the same behavior, the following studies were done with RumC1 only. We followed by fluorescent microscopy the incorporation of another DNA dye, the SYTOX green, that is also unable to cross undamaged membranes. While maximum fluorescence intensity was quickly detected with nisin after 10 min treatment at 5xMIC and decreased over time as DNA leaked out from permeabilized cells, the first significant fluorescence signals were only detected after 30 min treatment with RumC1 and the fluorescence intensity per cell surface increased significantly with time exposure from this point (Figure S3A and S3B). Additionally, we measured the impact of RumC1 on the integrity of *C. perfringens* cells by flow cytometry. After 15 min, and compared to untreated cells, a shift toward smaller particles was measured which then drastically increased with time and was in direct relation to the cell lysis observed and described above (Figure S3C). Interestingly, we previously showed that RumC1 treatment does not induce any cells permeabilization on *C. perfringens* when using cells in stationary phase.[14] Taking the present results into account, this observation much likely suggests that RumC might only be active on dividing cells. To confirm this hypothesis, we assayed the ability of RumC1 to kill *C. perfringens* cells either in log or stationary phase. RumC1 was able to kill more than 99% of the cells in log phase initially present in the culture after 1 h and no surviving cells were detected after 6 h treatment at 5xMIC (Figure S4). Conversely, no killing effect was observed on cells in stationary phase even after 48 h treatment with concentrations up to 10xMIC validating our initial hypothesis. Finally, and as we have previously shown that RumC1 was able to inhibit the energetically dependent synthesis pathways of the four macromolecules,[15] we undertook the measurement by bioluminescent assay on *C. perfringens* of the intracellular and extracellular ATP content after exposure to RumC isoforms (Figure 2B). After 15 min treatment with three different doses of each

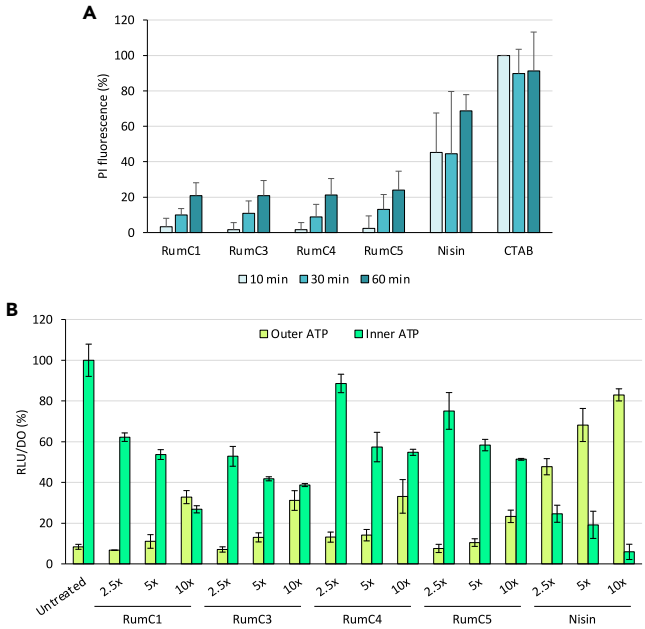

Figure 2. Mode of action of RumC isoforms

(A and B) *C. perfringens* cells in early log phase were treated with RumC isoforms, the well-characterized pore-forming RiPP nisin, or left untreated (negative control) in anaerobic condition at 37°C. Experiments were done in independent triplicates.

(A) After 10, 30, and 60 min of exposure at 5xMIC, cells were stained with propidium iodide (PI) and fluorescent signal (excitation 530 nm, emission 617 nm) was acquired. PI stains DNA but is unable to cross undamaged membrane. Cells incubated with cetyltrimethylammonium (CTAB) were used as positive control indicating maximum lysis.

(B) Cells were treated with 2.5x, 5x, and 10x MIC for each condition. After 15 min treatment, the ATP present in the extracellular media (outer ATP) was measured by bioluminescence, then cells were lysed, and the ATP content was measured again. The inner ATP content was deduced from the difference between ATP content in the extracellular media before and after cell lysis. Relative Light Units (RLU) are expressed as percentages normalized by the value of the inner ATP content of untreated cells.

isoform, and in contrast to treatment with nisin, a pore-forming bacteriocin causing a drastic increase in outer ATP due to cell leakage, inner ATP decreased in a dose dependent manner while outer ATP increased slightly. This observation corroborates that RumC isoforms exhibit a similar likely intracellular antibacterial mode of action with a non-porogenic effect leading to ATP depletion, cell death and subsequent lysis.

RumC isoforms have no synergistic effect on each other

From an evolutionary standpoint, we can wonder why *R. gnavus* E1 has maintained 5 isoforms of RumC in its genome. This led us to explore a potential synergetic effect between them. We first studied the effect of each pair of combinations and the five isoforms together in an equimolar ratio on *E. coli* and vancomycin-resistant *Enterococcus faecalis*. The most efficient combinations, i.e., those exhibiting a Minimal Inhibitory Equimolar Concentration (MIEC) lower or equal to the MIC of the most efficient isoform alone (lowest MIC/MIEC ≥ 1), were then further explored. For example, RumC3 and RumC5 have respective MICs of 16.6 and 6.2 μM on vancomycin-resistant *E. faecalis* (Table 1). When combined to a 1:1 M ratio, their MIEC is 6.2 μM - corresponding to 3.1 μM of RumC3 plus 3.1 μM of RumC5 — which is equal to the lowest MIC of the pair (Table 3). Despite the surprisingly non-synergistic effect of a combination with all 5 isoforms, such strategy has nevertheless revealed four interesting combinations, i.e., C1-C5, C2-C5, C3-C5 and C4-C5 on vancomycin-resistant *E. faecalis*, all including the RumC5 isoform. To conclude for a possible synergy, we picked the combination C1-C5 and C3-C5 for further characterization on vancomycin-resistant *E. faecalis* and *C. perfringens* by checkerboard assay that consists in double serial dilutions of two antimicrobials (Tables S1–S3). The MIC of each antimicrobial is determined alone or in combination, allowing the discrimination of antagonist, additive (or neutral) and synergistic activities. Only additive effects were identified with the C1-C5 combination on vancomycin-resistant *E. faecalis*. Consistently, we also detected an additive effect for the C1-C5 pair on *C. perfringens*, although the low Fractional Inhibitory Indexes (FICi) could suggest a slight synergetic effect (Tables S1). However, no FICi values indicates a potential synergetic effect on *C. perfringens* for the C3-C5 pair which undoubtfully displays an additive effect (Table S2). Some combinations exhibit an MIC/MIEC ratio of 0.5, which is not surprising since individual MICs on vancomycin-resistant *E. faecalis* cover a wide range depending on the isoform (Tables 3 and S3). For example, RumC1 and RumC4 have MICs of 3.1 and 25 μM, respectively. Their MIEC equals 6.25 μM, meaning that a concentration of 3.1 μM of RumC1 is still necessary to inhibit the growth of vancomycin-resistant *E. faecalis* even in the presence of RumC4. Some MIC/MIEC ratios were lower than 0.5. This is the case for the C1-C2 pair, which leads to an MIEC value of 9.5 μM. Such a result suggests a possible competition between the isoforms for the same molecular target or receptor. Regarding *E. coli*, neither inhibition nor synergism were found with any combination of the RumC isoforms (not shown).

Table 3. Synergistic studies on RumC isoforms

	Minimal inhibitory equimolar concentration (MIEC, μM)	Lowest MIC/MIEC
C1 + C2	9.5	0.3
C1 + C3	6.25	0.5
C1 + C4	6.25	0.5
C1 + C5	3.12	1
C2 + C3	50	0.3
C2 + C4	>100	<0.25
C2 + C5	6.25	1
C3 + C4	25	0.7
C3 + C5	6.25	1
C4 + C5	6.25	1
C1 + C2 + C3 + C4 + C5	9.3	0.3

Vancomycin-resistant *E. faecalis* was treated with equimolar mixtures of RumC isoforms. Minimal Inhibitory Equimolar Concentration (MIEC) was determined in the same manner as MICs except it corresponds to the addition of the concentrations of the different RumC isoforms. Then we calculated the ratio of the lowest MIC of the two isoforms by MIEC (see Tables S1–S3). A ratio ≥ 1 suggests an additive or synergistic effect whereas a ratio ≤ 0.5 indicate a neutral or antagonist effect.

RumC1 displays a species-specific synergetic effect with distinct conventional antibiotics targeting the cell wall synthesis

In parallel, the synergistic potential of RumC with conventional antibiotics was also explored, a strategy commonly employed with antimicrobial peptides in therapeutics. We studied combinations with a selection of antibiotics exhibiting different modes of action such as inhibition of nucleic acids synthesis (i.e., metronidazole, novobiocin, nalidixic acid, gemifloxacin, ciprofloxacin, rifampicin), translation (i.e., mupirocin, tetracycline, kanamycin, chloramphenicol, streptomycin), cell wall synthesis (i.e., fosfomycin, ampicillin, amoxicillin, imipenem, vancomycin), and inducing a membrane depolarization (i.e., valinomycin, gramicidin) or a membrane disruption (i.e., colistin, polymyxin B, nisin). As all isoforms display a similar mode of action and since RumC1 is the isoform exhibiting the lowest MICs, we focused this study on combination of conventional antibiotics with RumC1. Four Gram positive pathogens were picked for checkerboard assays: methicillin-resistant *Staphylococcus aureus*, *C. perfringens*, vancomycin-resistant *E. faecalis* and *S. pneumoniae*. Surprisingly, we found species-dependent results, where the same combination can exert different effects depending on the strain but also on the antibiotic used (Table 4). First, only one antagonist combination was found with mupirocin on methicillin-resistant *S. aureus* while no synergy was found with any antibiotics inhibiting translation, DNA or RNA synthesis. With respect to genome dynamics-inhibiting antibiotics, novobiocin has an intriguing synergistic effect with RumC1 on *S. pneumoniae,* whereas ciprofloxacin exerts a synergistic effect on vancomycin-resistant *E. faecalis* and a not well-defined effect (i.e., at the edge of additive or synergistic) on methicillin-resistant *S. aureus*. Of note, similarly to ciprofloxacin, a not well-defined effect was observed with membrane-targeting antibiotics (i.e., colistin and polymyxin B) via depolarization or disruption against both drug-resistant strains. Finally, the most interesting synergistic effects of RumC1 were found yet against methicillin-resistant *S. aureus* and vancomycin-resistant *E. faecalis* with antibiotics inhibiting cell wall synthesis (e.g., ampicillin, amoxicillin …) opening the way to a new therapeutic strategy (Tables S4–S7).

RumC isoforms are all safe and exhibit beneficial properties for human cells

Efficacy for counteracting a disorder is not the only characteristic required when developing a therapeutic molecule - or a combination of molecules - for human health; it must be safe as well. Therefore, we evaluated the cytotoxic activity of RumC isoforms on human epithelial cell lines corresponding to the small intestine (Caco 2, Figure 3A), kidney (A498, Figure 3B), and liver (HepG2, Figure 3C), respectively. All five RumC isoforms were tested and did not impact human cell viability, as indicated by metabolic activity measured via the resazurin assay, even at high concentration [IC_{50} (median inhibitory concentration) > 100 μM]. Additionally, no hemolysis of human erythrocytes was recorded for all isoforms [EC_{50} (median effective concentration) > 100 μM, Figure 3D]. We also evaluated the effect of the combination between RumC1 and amoxicillin identified as one of the potential therapeutic leads, in equal amounts. No cytotoxic effect was observed on the three cell lines even with a mixture of 100 μM of RumC1 with 100 μM of amoxicillin (Figures 3A–3C).

Previously, we showed that RumC1 has a general anti-inflammatory effect (i.e., not only linked to bacterial molecules but also IL1-β mediated one).[19] We therefore investigated whether and to which extent the other isoforms also possess this activity using the HeLa eLUCidate TLR4/IL-8 reporter cell line (Figure 3E). In this cell line, the *Renilla* luciferase expression is directly related to the inflammatory signaling artificially induced with IL-1β. For all five isoforms, exposure to 25 μM results in 25–40% inhibition of the inflammatory response. Above a concentration of 50 μM, and stably up to 100 μM, the inflammatory inhibitory response observed for RumC2, C3 and C4 did not increase significantly. As previously observed for RumC1,[19] RumC5 showed a similar and strong activity with a decrease in inflammatory response of 50–65% in a dose-dependent manner. Furthermore, the anti-inflammatory effect of RumC1 in combination with amoxicillin was maintained with up to

Table 4. Synergistic studies on RumC isoforms and conventional antibiotics

Antibiotic	Metabolic pathway targeted	Methicillin -resistant *S. aureus*	*C. perfringens*	Vancomycin – Resistant *E. faecalis*	*S. pneumoniae*
Mupirocin	Translation	A	–	–	N
Tetracycline	Translation	N	N	–	N
Kanamycin	Translation	–	–	–	N
Chloramphenicol	Translation	N	N	N	N
Streptomycin	Translation	N	–	–	N
Metronidazole	Nucleic acids synthesis	N	–	–	–
Novobiocin	DNA synthesis	N	N	N	S
Nalidixic acid	DNA synthesis	N	N	–	–
Gemifloxacin	DNA synthesis	N	N	–	
Ciprofloxacin	DNA synthesis	S/N	N	S	N
Rifampicin	RNA synthesis	N	N	N	
Fosfomycin	Cell wall synthesis	S	–	–	–
Ampicillin	Cell wall synthesis	S	N	S	N
Amoxicillin	Cell wall synthesis	S	N	S/N	N
Imipenem	Cell wall synthesis	S	N	S/N	N
Vancomycin	Cell wall synthesis	N	N	S	N
Valinomycin	Membrane depolarization	–	N	–	N
Gramicidin	Membrane depolarization	–	N	S/N	
Colistin	Membrane disruption	S/N	–	–	–
Polymyxin B	Membrane disruption	S/N	–	–	–
Nisin	Membrane disruption	N	N	N	N

MICs of conventional antibiotics and RumC1 were determined alone or in combination by a double serial dilution. Then Fractional Inhibitory Concentrations (FICs) were determined as follow: FIC C1= (MIC C1 in combination with antibiotic)/MIC C1 alone; FIC antibiotic = (MIC antibiotic in combination with C1)/MIC antibiotic alone; FIC index (FICi) = FIC C1 + FIC antibiotic for each well with a growth inhibition (see Tables S4–S7). The combination was qualified as synergistic (S) if one FICi $\leq$0.5, neutral or additive (N) when 0.5 < FICi <4, (S/N) when the result is ambiguous, or antagonist (A) if one FICi >4. "-" indicates an MIC of the antibiotic alone >100 μM and thus not tested with the peptide. Each combination was assayed twice for each specie.

42 and 61% inhibition of the anti-inflammatory response at doses of 50 and 100 μM, respectively (Figure 3E). Finally, it is noteworthy that despite its lack of antibacterial activity, RumC2 exhibits an interesting anti-inflammatory effect.

A pocket-like structural region of RumC is crucial for antibacterial activity

Since RumC2 shares between 75 and 82% sequence identity and shows a conserved thioether network with the other natural isoforms (Figure 1D), its lack of antibacterial activity observed on the strains assayed was not expected. Thus, we tried to figure out which key residue(s) is (are) crucial for the antibacterial activity of RumCs. Among the 9 residues that are not conserved between RumC1 and RumC2 (see Figure 4A), four belong to different groups of amino acids (i.e., non-polar, polar, basic or acidic) in the two peptide sequences at positions 4, 8, 12 and 44. The superimposition of the RumC1 3D-structure (PDB: 6T33) and the RumC2 3D-model revealed that 3 out of these 4 residues (i.e., at positions 4, 12 and 44) are located in a relatively open structural pocket-like region for RumC1, whereas the basic and acidic side chains found in RumC2 at these positions seem to generate steric hindrance restricting this hypothetical cavity (Figure 4B). Figure S5A shows that the structural models of RumC2-5 are very similar to the 3D-NMR structure of RumC1. This result strongly suggests that the thioether network, strictly conserved among the 5 RumC isoforms, imposes a very close folding of the 5 peptides Nevertheless, surface charge analysis clearly revealed an overall neutral, slightly positive environment of the pocket-like structure for RumC1, C3, C4 and C5, while the Glu12 and Lys4 found on the RumC2 isoform tend to charge (positively and negatively) the surface of the corresponding region (Figure S5B). This observation allowed us to hypothesize a specific role of these residues and guided us for the generation of a rational library of single and multiple substitution variants, both in RumC1 or RumC2, to either decrease or increase their antibacterial activity against a representative panel of seven RumC1-sensitive strains (Table 5). First, at position 8, RumC2 carries a non-polar glycine residue unlike the other isoforms that contain a polar residue (serine or threonine). As anticipated, the single S8G mutation in RumC1 does not significantly affect its antibacterial activity (Table 5). Indeed, and rationally, the structures of RumC1 and RumC2 show that this residue is quite distant from the pocket-like region defined by residues 4, 12, and 44 (Figure 4B). Second, as RumC2 is the only isoform with a glutamic acid instead of an alanine at position 12 - involved in one of the four sactionine-bridges of the matured peptide - we individually studied the influence of this residue on the antibacterial activity. A substitution of the

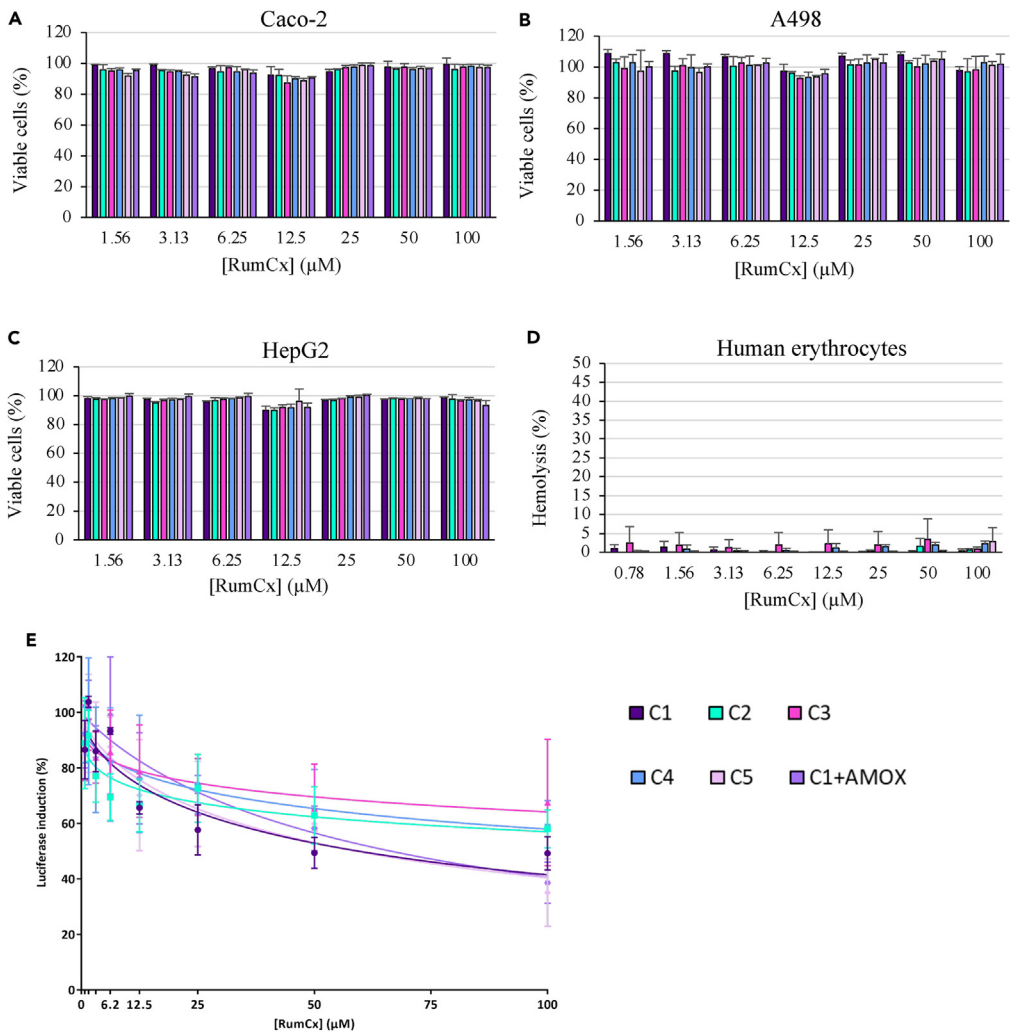

Figure 3. Activity of RumC isoforms alone or in combination on eukaryotic cells

(A–C) Human cell lines (A–C) and erythrocytes (D) were incubated with increasing concentrations of RumC isoforms. (A–C) Cells were incubated with resazurin and conversion into fluorescent resorufin was monitored to measure metabolic activity as an indicator of cell viability. Untreated cells were used as a positive control. Caco-2 (A), A498 (B) and HepG2 (C) were used as models of human small intestinal, kidney, and liver epithelial cells, respectively.

(D) Hemoglobin release was measured to monitor the lytic potency of RumC isoforms. Cells incubated with Triton X-100 were used as a positive control for maximum lysis, untreated cells were used as a negative control.

(E) The anti-inflammatory activities of RumC isoforms was evaluated using HeLa eLUCidate TLR4/IL-8 cells incubated with IL-1β and then treated with increasing concentration of RumC isoforms. Luciferase luminescence, induced by pro-inflammatory transcription factors, was measured. Untreated cells were used to determine the maximum of luciferase induction. (A-C, E) Additionally the effects of a combination of RumC1 with amoxicillin at a 1:1 M ratio was assayed, e.g., 100 µM equals a combination of 100 µM of RumC1 and 100 µM of amoxicillin. (A-E) Experiments were done in triplicates.

alanine into glutamic acid at position 12 in RumC1 (corresponding to the RumC1-A12E variant, Figures 4A and 4B) profoundly alters its antimicrobial activity, resulting in at least ~100-fold increase in its MIC value against RumC1-sensitive strains (Table 5). Then, to assess whether the removal of this glutamic acid could help to restore the antibacterial activity of RumC2, we generated the corresponding RumC2-E12A variant. This substitution partially restored the activity toward *V. alginolyticus*, *B. subtilis*, and *L. monocytogenes* with a 3-to-30-fold increase in MICs compared to RumC1's MIC. However, *C. perfringens*, *S. pneumoniae*, and *E. faecalis* remained resistant to the RumC2-E12A variant. This led us to study the other residues that differ in RumC2. In position 4, there is a basic residue (i.e., lysine) whereas all the other isoforms have a non-polar residue (i.e., either a valine or an isoleucine) (Figures 4A, 4B, and S5B). For the single RumC1-V4K variant, two completely different behaviors have been found depending on the seven species tested (Table 5). Indeed, there is almost no impact on the MIC or even a significant improvement for *B. subtilis, L. monocytogenes* and *V. alginolyticus*, while the MIC against *C. perfringens, S. pneumoniae* and *E. faecalis* appears to be strongly increased. It should also be noted that these bacterial species are the same ones for which the E12A mutation on RumC2 did not restore the activity. Surprisingly, the very low MIC obtained for the RumC1-V4K variant against the *E. coli* K-12*Δimp4213* mutant strain

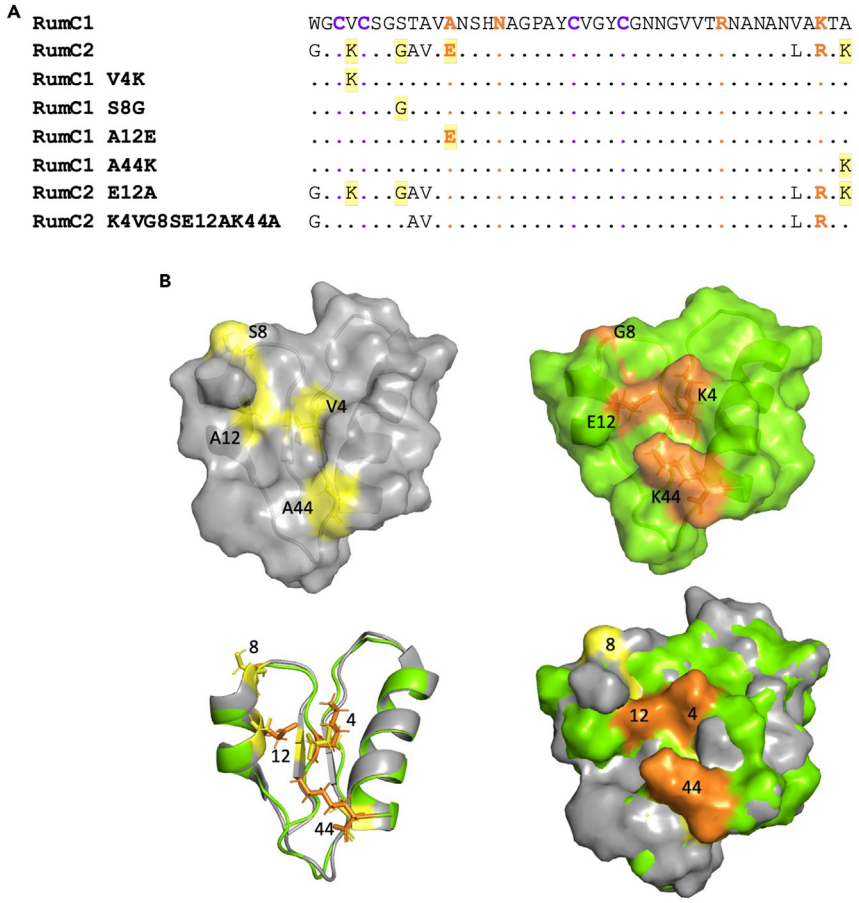

Figure 4. RumC1 and RumC2 site-directed mutagenesis

(A) Sequence alignment of RumC1 and RumC2. Purple and orange indicates cysteine and amino acids involved in sactionine bridges whereas yellow highlights targeted amino acid for site-directed mutagenesis.

(B) Structural superimposition of RumC1 and RumC2. The 3D structure of RumC1 (PDB: 6T33) appears in gray and the 3D Rosetta structural model of RumC2 appears in green. Residue differences for the position 4, 8, 12, and 44 are colored in yellow and orange for RumC1 and RumC2, respectively.

(i.e., 3.6 μM) has never been reached for any of the 5 natural RumC isoforms, opening the way to design RumC-like peptides active against Gram negative bacteria by playing on the nature of the residue at this position. Finally, the last targeted position 44 shows for RumC2 a basic residue, i.e., lysine, whereas RumC1, 3, and 5 all have a non-polar alanine and RumC4 has a polar serine (see Figures 4A, 4B, and S5B). As shown in Figure 2C, the single A44K mutation do not significantly disturb the efficacy of RumC1. At this stage, we combined the different mutations on RumC2, generating a quadruple variant (RumC2-K4V/G8S/E12A/K44A) to confirm if such combination could explain the differences between RumC1 and RumC2. Remarkably, the antibacterial activity of the RumC2 quadruple variant against all pathogenic strains tested was significantly improved with comparable or even better MICs than RumC1 (Table 5). Nevertheless, and considering that the single S8G and A44K mutations in RumC1 do not substantially affect its efficacy, we hypothesize that the activity observed for the RumC2-K4V/G8S/E12A/K44A variant is mainly dictated by the K4V and E12A substitutions. Overall, these results strongly suggest that the nature of residues at positions 4 and 12 play a key role in the antimicrobial mechanism of RumC isoforms.

DISCUSSION

In this work, the five mature RumC isoforms were successfully produced by using the heterologous co-expression protocol previously established for RumC1. Importantly, this system generates the 5 RumC peptides with the same level of post-translational modifications as does *R. gnavus* E1 in the context of symbiosis within a mammalian host. This allowed us to study the functional properties of each RumC peptide individually for comparison. Despite the strong sequence identity between the two paralogous sactisynthases RumMc1and RumMc2 (96%), we found that RumMc1 is more adapted to introduce the correct four thioether crosslinks on all isoforms and to produce their mature forms with higher yields. We have previously shown that the leader peptide of RumC1 is crucial for the maturation by RumMc1.[14] Since the leader sequences of RumC1 and RumC2 are identical, the maturation defect of RumC2 by RumMc2 is surprising. In addition, this was not expected

Table 5. Antibacterial activity of the site-directed mutants of RumC1 and RumC2

MIC RumC (μM)	*Clostridium perfringens*	*Bacillus subtilis*	*Streptococcus pneumoniae*	*Enterococcus faecalis*	*Listeria monocytogenes*	*Vibrio alginolyticus*	Δ *Escherichia coli*
C1 WT	0.8	0.1	0.8	3.1	0.8	0.06	18.7
C1 V4K	41.7	0.1	37.5	28.1	0.5	0.04	3.6
C1 S8G	1	0.03	2.1	3.1	0.5	0.04	25
C1 A12E	R	9.3	R	100	100	25	66.7
C1 A44K	3	0.04	2.7	2.8	0.04	0.04	8.3
C2 WT	R	R	R	R	R	R	75
C2 E12A	R	3.1	R	R	4.2	0.2	6.2
C2 K4V G8S E12A	6.2	0.07	6.2	10.4	0.2	0.01	9.4
C2 K4V G8S E12A K44A	1.8	0.06	6.6	12.5	0.3	0.06	12.5

MICs of RumC1-WT, RumC2-WT and their corresponding variants. MICs were determined in independent triplicates.

since the *in vitro* maturation of RumC2 by RumMc2 has been previously reported.[13,23] This is even more surprising considering the promiscuity of the genes encoding sactisynthases and peptide isoforms, but also the dependence on the same promoter. Indeed, the *rumMc2*, *rumC2*, and *rumC3* genes are adjacent, but RumMc2 does not efficiently mature RumC2, whereas RumC3 or RumC1 are processed by RumMc2. Consequently, we may hypothesize that the maturation of the 5 isoforms and the genes proximity (between sactisynthases and peptides) appear not to be correlated to specific couple.

Since all isoforms are naturally produced by *R. gnavus* E1, we had anticipated that all RumC peptides would exhibit antibacterial activities. However, our results show that they possess different biological properties. Of most importance, is the lack of antibacterial activity of RumC2 on the diversity of bacterial pathogenic strains tested, but interestingly, this observation guided us to the residues and broadly to a region of RumC that appears essential for antibacterial activity or bacterial cell penetration. Specifically, from a molecular point of view, it appears from the site-directed mutagenesis analysis that the pocket-like structure involving residues 4 and 12 (see Figure 4B) is crucial for the antibacterial activity. Of most importance in this cavity is the presence of an alanine residue at position 12 in all RumC isoforms except in RumC2, for which the presence of a glutamic acid prevents the antibacterial activity, either by a binding defect to the intracellular target or merely by an inability to penetrate the cell. Furthermore, it also appears that this region, is relatively well-conserved in terms of charge on RumC1 and C3 to C5, but differs on RumC2, reinforcing the idea that this pocket-like region where residues 4 and 12 are located is essential. Concerning RumC2, despite its lack of antibacterial activity, the peptide surprisingly retains an anti-inflammatory activity, allowing us to conclude that the residues targeted for site-directed mutagenesis, and of importance for antibacterial activity, do not seem to be involved in the activities on eukaryotic cells.

In addition, and interestingly, the results obtained here on the activity tests performed on the Gram-negative *V. alginolyticus* and *E. coli* K-12Δ*imp4213* strains, contrast with the results obtained in our previous studies where RumCs seemed to be limited to Gram-positive targets. According to these results, the most likely interpretation seems to be related to the lack or lower amount of LPS on the surface of the bacterial envelope, so that RumCs can penetrate the bacteria and reach their molecular target, with LPS obviously playing a barrier role. This observation extends the interest of RumCs for their ability to target new LPS-poor pathogenic Gram-negative bacteria. Beyond an informative scale on the mechanism of action of these sactipeptides, this discovery also opens the way to the design of optimized peptides broadening for example the spectrum of specificity of RumCs or even aiming to increase their efficacy.

Otherwise, two hypotheses were initially formulated to explain the interest for a bacterium from the human gut microbiome to produce 5 relatively conserved AMP isoforms: these isoforms would exhibit different antibacterial activity spectra or more plausibly they would have a synergistic effect. Our experiments showed that neither of the two hypotheses was the right one, leaving this fundamental question open. Nevertheless, we were able to show that RumCs (except RumC2) all have a selective killing action toward dividing cells, not caused by pore formation but probably related to energy depletion, eventually leading to cell lysis, but most importantly suggesting that the four isoforms present the same mode of action. At this stage, the only hypothesis for the lack of synergy between isoforms is based on a well-known phenomenon in therapeutics where antibiotic molecules exhibiting an identical mode of action have no synergistic effect, which seems to be the natural case for RumCs. Hence, the synergies observed between RumCs and cell wall-targeting antibiotics, such as ampicillin or amoxicillin, against antibiotic-resistant strains is a very interesting point which confirms our previous conclusion that antimicrobial synergies are very often observed when the modes of action are different. Indeed, ampicillin, amoxicillin or even imipenem target the cell wall, and conversely to the initial results obtained on the mode of action of RumCs, we can hypothesize that inhibition of cell wall synthesis potentiates RumCs activity. Furthermore, based on safety tests, it appears that a combination with amoxicillin is safe and maintains the anti-inflammatory effect obtained with RumC isoforms alone. Obviously, even if those combinations seem promising from a therapeutic point of view, further (pre)

clinical investigations are necessary, knowing that combinations have the strong advantage of limiting the emergence of resistance, of limiting the amount of RumCs necessary (not yet produced on an industrial scale), while maintaining the advantages of such sactipeptide.

To conclude, we demonstrate in this study the propensity of both sactisynthases RumMc1 and RumMc2 to perform sactionine cross-links despite a more effective maturation by RumMc1. Regarding the biological functions, all the isoforms except RumC2 display an antibacterial activity on the same spectrum, whereas RumC2 seems to be active only on eukaryotic cells. No antibacterial synergistic effect was found between isoforms as they much likely exhibit the same mechanism of action; however, a combination of RumC1 with conventional antibiotics were found to be a potential therapeutic lead to fight methicillin-resistant *S. aureus* and vancomycin-resistant *E. faecalis*. Finally, rational site-directed mutagenesis pointed out the residues that are determinant for the antimicrobial activity, thus paving the way for the development of RumC-like molecules.

Limitation of the study

The gut microbiota includes a variety of bacterial species. Yet, in this study, the peptides were tested only on a limited number of laboratory available strains. The inactivity of RumC2 on the strains tested does not exclude the possibility that it might be working *in vivo* on an untackled target. Moreover, unlike RumC1, the activity and safety of RumC3-C5 were evaluated *in vitro* without the confirmation *in vivo* using an animal model of infection.

STAR★METHODS

Detailed methods are provided in the online version of this paper and include the following:

- KEY RESOURCES TABLE
- RESOURCE AVAILABILITY
  - Lead contact
  - Materials availability
  - Data and code availability
- EXPERIMENTAL MODEL AND SUBJECT DETAILS
  - Bacterial strains
  - Cell lines
- METHOD DETAILS
  - Heterologous expression and purification of fully mature RumC1-5
  - Mutant productions
  - Nano-LC-MS/MS analyses
  - MS data analyses
  - Structure prediction
  - Membrane permeability assay
  - Flow cytometry
  - Antibiotics
  - MIC determination
  - ATP bioluminescent assays
  - Minimal equimolar inhibitory concentration (MEIC) determination
  - Checkerboard assay
  - Time-kill kinetics assay
  - Hemolytic activity assay
  - Cytotoxic activity assay
  - Anti-inflammatory activity
- QUANTIFICATION AND STATISTICAL ANALYSIS

SUPPLEMENTAL INFORMATION

Supplemental information can be found online at https://doi.org/10.1016/j.isci.2023.107563.

ACKNOWLEDGMENTS

This study was supported by a grant from the French National Agency for Research ("Agence Nationale de la Recherche") through the "Projet de Recherche Collaboratif" *RUMisBAC* (ANR-20-CE44-0021) and partly supported by the Labex ARCANE (CBH-EUR-GS, ANR-17-EURE-0003) and by the FrenchBIC CNRS network. We would also like to thank Nicolas Vidal from Yelen Analytics for providing Yelen buffer.

AUTHOR CONTRIBUTIONS

L.S., C.B., L.D.M., and V.D. were in charge of the site-directed mutagenesis, RumC isoforms productions, variant productions, and purifications; L.S., C.R., I.V., A.A., and E.C.D. managed activity and synergy experiments; C.R., C.N., G.B., M.M., and M.L. performed the mechanistic analyses and safety assays; S.K.F. was in charge of the mass spectrometry experiments and related data interpretation; V.D., P.C., and M.L. established the structural models; A.B., N.C., and M.B. contributed to the manuscript writing, critical review and comments; P.P., J.P., V.D., and M.L. were involved in the design and coordination of the study; C.R., L.S., V.D., and M.L. were in charge of the data acquisition, data interpretation, and manuscript writing; V.D. and M.L. were in charge of the correspondence with the editorial board.

DECLARATION OF INTERESTS

The authors declare that the research was conducted in the absence of any commercial or financial relationships that could be constructed as a potential conflict of interest.

INCLUSION AND DIVERSITY

We support inclusive, diverse, and equitable conduct of research.

Received: March 3, 2023
Revised: June 6, 2023
Accepted: August 2, 2023
Published: August 6, 2023

REFERENCES

1. O'Neill, J. (2016). Tackling Drug-Resistant Infections Globally Final Report and Recommendations (Publ. Html *The Review on Antimicrobial Resistance*).
2. Arnison, P.G., Bibb, M.J., Bierbaum, G., Bowers, A.A., Bugni, T.S., Bulaj, G., Camarero, J.A., Campopiano, D.J., Challis, G.L., Clardy, J., et al. (2013). Ribosomally synthesized and post-translationally modified peptide natural products: overview and recommendations for a universal nomenclature. Nat. Prod. Rep. *30*, 108–160. https://doi.org/10.1039/C2NP20085F.
3. Ali, A., Happel, D., Habermann, J., Schoenfeld, K., Macarrón Palacios, A., Bitsch, S., Englert, S., Schneider, H., Avrutina, O., Fabritz, S., and Kolmar, H. (2022). Sactipeptide Engineering by Probing the Substrate Tolerance of a Thioether-Bond-Forming Sactisynthase. Angew Chem. Int. Ed. Engl. *61*, e202210883. https://doi.org/10.1002/anie.202210883.
4. Clark, K.A., Covington, B.C., and Seyedsayamdost, M.R. (2021). Biosynthesis-Guided Discovery of Enteropeptins, Unusual Sactipeptides Containing an N-Methylornithine. Preprint at ChemRxiv. https://doi.org/10.26434/chemrxiv-2021-jnv18.
5. Rousselot-Pailley, P., and Iranzo, O. (2023). Peptide and Protein Engineering for Biotechnological and Therapeutic Applications (WORLD SCIENTIFIC). https://doi.org/10.1142/13005.
6. Kawulka, K., Sprules, T., McKay, R.T., Mercier, P., Diaper, C.M., Zuber, P., and Vederas, J.C. (2003). Structure of Subtilosin A, an Antimicrobial Peptide from *Bacillus s ubtilis* with Unusual Posttranslational Modifications Linking Cysteine Sulfurs to α-Carbons of Phenylalanine and Threonine. J. Am. Chem. Soc. *125*, 4726–4727. https://doi.org/10.1021/ja029654t.
7. Lee, H., Churey, J.J., and Worobo, R.W. (2009). Biosynthesis and transcriptional analysis of thurincin H, a tandem repeated bacteriocin genetic locus, produced by Bacillus thuringiensis SF361. FEMS Microbiol. Lett. *299*, 205–213. https://doi.org/10.1111/j.1574-6968.2009.01749.x.
8. Liu, W.-T., Yang, Y.-L., Xu, Y., Lamsa, A., Haste, N.M., Yang, J.Y., Ng, J., Gonzalez, D., Ellermeier, C.D., Straight, P.D., et al. (2010). Imaging mass spectrometry of intraspecies metabolic exchange revealed the cannibalistic factors of Bacillus subtilis. Proc. Natl. Acad. Sci. USA *107*, 16286–16290. https://doi.org/10.1073/pnas.1008368107.
9. Rea, M.C., Sit, C.S., Clayton, E., O'Connor, P.M., Whittal, R.M., Zheng, J., Vederas, J.C., Ross, R.P., and Hill, C. (2010). Thuricin CD, a posttranslationally modified bacteriocin with a narrow spectrum of activity against Clostridium difficile. Proc. Natl. Acad. Sci. USA *107*, 9352–9357. https://doi.org/10.1073/pnas.0913554107.
10. Mo, T., Ji, X., Yuan, W., Mandalapu, D., Wang, F., Zhong, Y., Li, F., Chen, Q., Ding, W., Deng, Z., et al. (2019). Thuricin Z: A Narrow-Spectrum Sactibiotic that Targets the Cell Membrane. Angew. Chem. Int. Ed. *58*, 18793–18797. https://doi.org/10.1002/anie.201908490.
11. Hudson, G.A., Burkhart, B.J., DiCaprio, A.J., Schwalen, C.J., Kille, B., Pogorelov, T.V., and Mitchell, D.A. (2019). Bioinformatic Mapping of Radical *S* -Adenosylmethionine-Dependent Ribosomally Synthesized and Post-Translationally Modified Peptides Identifies New Cα, Cβ, and Cγ-Linked Thioether-Containing Peptides. J. Am. Chem. Soc. *141*, 8228–8238. https://doi.org/10.1021/jacs.9b01519.
12. Duarte, A.F.d.S., Ceotto-Vigoder, H., Barrias, E.S., Souto-Padrón, T.C.B.S., Nes, I.F., Bastos, M.d.C.d.F., and do, C. de F. (2018). Hyicin 4244, the first sactibiotic described in staphylococci, exhibits an anti-staphylococcal biofilm activity. Int. J. Antimicrob. Agents *51*, 349–356. https://doi.org/10.1016/j.ijantimicag.2017.06.025.
13. Balty, C., Guillot, A., Fradale, L., Brewee, C., Boulay, M., Kubiak, X., Benjdia, A., and Berteau, O. (2019). Ruminococcin C, an anti-clostridial sactipeptide produced by a prominent member of the human microbiota Ruminococcus gnavus. J. Biol. Chem. *294*, 14512–14525. https://doi.org/10.1074/jbc.RA119.009416.
14. Chiumento, S., Roblin, C., Kieffer-Jaquinod, S., Tachon, S., Leprètre, C., Basset, C., Aditiyarini, D., Olleik, H., Nicoletti, C., Bornet, O., et al. (2019). Ruminococcin C, a promising antibiotic produced by a human gut symbiont. Sci. Adv. *5*, eaaw9969. https://doi.org/10.1126/sciadv.aaw9969.
15. Roblin, C., Chiumento, S., Bornet, O., Nouailler, M., Müller, C.S., Jeannot, K., Basset, C., Kieffer-Jaquinod, S., Couté, Y., Torelli, S., et al. (2020). The unusual structure of Ruminococcin C1 antimicrobial peptide confers clinical properties. Proc. Natl. Acad. Sci. USA *117*, 19168–19177. https://doi.org/10.1073/pnas.2004045117.
16. Bushin, L.B., Covington, B.C., Rued, B.E., Federle, M.J., and Seyedsayamdost, M.R. (2020). Discovery and Biosynthesis of Streptosactin, a Sactipeptide with an Alternative Topology Encoded by Commensal Bacteria in the Human Microbiome. J. Am. Chem. Soc. *142*, 16265–16275. https://doi.org/10.1021/jacs.0c05546.
17. Caruso, A., and Seyedsayamdost, M.R. (2021). Radical SAM Enzyme QmpB Installs Two 9-Membered Ring Sactionine Macrocycles during Biogenesis of a Ribosomal Peptide Natural Product. J. Org. Chem. *86*, 11284–11289. https://doi.org/10.1021/acs.joc.1c01507.
18. Pujol, A., Crost, E.H., Simon, G., Barbe, V., Vallenet, D., Gomez, A., and Fons, M. (2011). Characterization and distribution of the gene cluster encoding RumC, an anti-Clostridium perfringens bacteriocin produced in the gut. FEMS Microbiol. Ecol. *78*, 405–415. https://doi.org/10.1111/j.1574-6941.2011.01176.x.
19. Roblin, C., Chiumento, S., Jacqueline, C., Pinloche, E., Nicoletti, C., Olleik, H., Courvoisier-Dezord, E., Amouric, A., Basset, C., Dru, L., et al. (2021). The Multifunctional Sactipeptide Ruminococcin C1 Displays

Potent Antibacterial Activity In Vivo as Well as Other Beneficial Properties for Human Health. Int. J. Mol. Sci. *22*, 3253. https://doi.org/10.3390/ijms22063253.

20. Sijmons, D., Guy, A.J., Walduck, A.K., and Ramsland, P.A. (2022). Helicobacter pylori and the Role of Lipopolysaccharide Variation in Innate Immune Evasion. Front. Immunol. *13*, 868225. https://doi.org/10.3389/fimmu.2022.868225.
21. Yokota, S.i., Ohnishi, T., Muroi, M., Tanamoto, K.i., Fujii, N., and Amano, K.i. (2007). Highly-purified *Helicobacter pylori* LPS preparations induce weak inflammatory reactions and utilize Toll-like receptor 2 complex but not Toll-like receptor 4 complex. FEMS Immunol. Med. Microbiol. *51*, 140–148. https://doi.org/10.1111/j.1574-695X.2007.00288.x.
22. Sampson, B.A., Misra, R., and Benson, S.A. (1989). Identification and characterization of a new gene of Escherichia coli K-12 involved in outer membrane permeability. Genetics *122*, 491–501. https://doi.org/10.1093/genetics/122.3.491.
23. Balty, C., Guillot, A., Fradale, L., Brewee, C., Lefranc, B., Herrero, C., Sandström, C., Leprince, J., Berteau, O., and Benjdia, A. (2020). Biosynthesis of the sactipeptide Ruminococcin C by the human microbiome: Mechanistic insights into thioether bond formation by radical SAM enzymes. J. Biol. Chem. *295*, 16665–16677. https://doi.org/10.1074/jbc.RA120.015371.
24. Song, Y., DiMaio, F., Wang, R.Y.-R., Kim, D., Miles, C., Brunette, T., Thompson, J., and Baker, D. (2013). High-Resolution Comparative Modeling with RosettaCM. Structure *21*, 1735–1742. https://doi.org/10.1016/j.str.2013.08.005.
25. Raman, S., Vernon, R., Thompson, J., Tyka, M., Sadreyev, R., Pei, J., Kim, D., Kellogg, E., DiMaio, F., Lange, O., et al. (2009). Structure prediction for CASP8 with all-atom refinement using Rosetta. Proteins *77* (*Suppl 9*), 89–99. https://doi.org/10.1002/prot.22540.
26. Jurrus, E., Engel, D., Star, K., Monson, K., Brandi, J., Felberg, L.E., Brookes, D.H., Wilson, L., Chen, J., Liles, K., et al. (2018). Improvements to the APBS biomolecular solvation software suite. Protein Sci. *27*, 112–128. https://doi.org/10.1002/pro.3280.
27. Schrödinger, L., and DeLano, W. (2020). PyMOL.
28. The European Committee on Antimicrobial Susceptibility Testing (2022). Breakpoint Tables for Interpretation of MICs and Zone Diameters. Version 12.0, 2022.
29. Chappelle, E.W., and Levin, G.V. (1968). Use of the firefly bioluminescent reaction for rapid detection and counting of bacteria. Biochem. Med. *2*, 41–52. https://doi.org/10.1016/0006-2944(68)90006-9.
30. Oyama, L.B., Girdwood, S.E., Cookson, A.R., Fernandez-Fuentes, N., Privé, F., Vallin, H.E., Wilkinson, T.J., Golyshin, P.N., Golyshina, O.V., Mikut, R., et al. (2017). The rumen microbiome: an underexplored resource for novel antimicrobial discovery. NPJ Biofilms Microbiomes *3*, 33. https://doi.org/10.1038/s41522-017-0042-1.
31. Tardy, A., Honoré, J.C., Tran, J., Siri, D., Delplace, V., Bataille, I., Letourneur, D., Perrier, J., Nicoletti, C., Maresca, M., et al. (2017). Radical Copolymerization of Vinyl Ethers and Cyclic Ketene Acetals as a Versatile Platform to Design Functional Polyesters. Angew. Chem. Int. Ed. *56*, 16515–16520. https://doi.org/10.1002/anie.201707043.
32. Benkhaled, B.T., Hadiouch, S., Olleik, H., Perrier, J., Ysacco, C., Guillaneuf, Y., Gigmes, D., Maresca, M., and Lefay, C. (2018). Elaboration of antimicrobial polymeric materials by dispersion of well-defined amphiphilic methacrylic SG1-based copolymers. Polym. Chem. *9*, 3127–3141. https://doi.org/10.1039/C8PY00523K.
33. Borie, C., Mondal, S., Arif, T., Briand, M., Lingua, H., Dumur, F., Gigmes, D., Stocker, P., Barbarat, B., Robert, V., et al. (2018). Enediynes bearing polyfluoroaryl sulfoxide as new antiproliferative agents with dual targeting of microtubules and DNA. Eur. J. Med. Chem. *148*, 306–313. https://doi.org/10.1016/j.ejmech.2018.02.030.

STAR★METHODS

KEY RESOURCES TABLE

REAGENT or RESOURCE	SOURCE	IDENTIFIER
Bacterial and virus strains		
Clostridium perfringens	American Type Culture Collection (ATCC)	ATCC 13124
Clostridium difficile	Leibniz Institute DSMZ Collection	DSMZ 1296
Listeria monocytogenes	Leibniz Institute DSM Collection	DSM 20600
Bacillus cereus	*Collection de l'Institut Pasteur*	CIP 5257
Bacillus subtilis	American Type Culture Collection (ATCC)	ATCC 6633
Streptococcus pneumoniae	A laboratory collection (Laboratoire de Microbiologie et Genetique Moleculaires - Center for Integrative Biology in Toulouse	R 1501
Vancomycin-resistant *Enterococcus faecalis*	Leibniz Institute DSMZ Collection	DSMZ 13591
Methicillin-resistant *Staphylococcus aureus*	American Type Culture Collection (ATCC)	ATCC BAA-1717
Vibrio alginolyticus	Leibniz Institute DSM Collection	DSM 2172
Helicobacter pylori	American Type Culture Collection (ATCC)	ATCC 43504
Escherichia coli	American Type Culture Collection (ATCC)	ATCC 8739
Pseudomonas aeruginosa	American Type Culture Collection (ATCC)	ATCC 9027
Acinetobacter baumanii	*Collection de l'Institut Pasteur*	CIP 110431
Δ Escherichia coli (imp4213)	*Collection de l'Institut Pasteur*	CIP 111272
Escherichia coli	Thermofischer scientific	BL21(DE3), cat# EC0114
Chemicals, peptides, and recombinant proteins		
Peptides RumC1-5/Mutants	Produced in the laboratory through heterologous expression in *E. coli BL21(DE3)*	–
Nisin from *Lactococcus lactis*	Sigma-Aldrich	Cat# 1414-45-5
Kanamycin	Sigma-Aldrich	K1876
Ampicillin	Sigma-Aldrich	A9393
Chloramphenicol	Sigma-Aldrich	R4408
Vitamin B1	Sigma-Aldrich	V-014
Iron Chloride $FeCl_3$	Sigma-Aldrich	157740
Magnesium sulfate MgSO4	Sigma-Aldrich	M7506
Glucose	Sigma-Aldrich	G8270
L-cysteine	Sigma-Aldrich	168149
IPTG	Sigma-Aldrich	I6758
Tris	Sigma-Aldrich	GE17-1321-01
Sodium chloride NaCl	Sigma-Aldrich	S9625
Maltose	Sigma-Aldrich	1375025
HEPES	Sigma-Aldrich	H3375
Acetonitrile	Sigma-Aldrich	34998
Trifluoroacetic acid	Sigma-Aldrich	302031
PBS	Sigma-Aldrich	P4474
Propidium iodide	Sigma-Aldrich	P4170
Mupirocin	Sigma-Aldrich	PHR2806
Metronidazole	Sigma-Aldrich	PHR1052

(*Continued on next page*)

Continued

REAGENT or RESOURCE	SOURCE	IDENTIFIER
Fosfomycin	Sigma-Aldrich	1286322
Tetracycline	Sigma-Aldrich	T3258
Novobiocin	Sigma-Aldrich	1475008
Amoxicillin	Sigma-Aldrich	1031503
Nalidixic acid	Sigma-Aldrich	N8878
Streptomycin	Sigma-Aldrich	S6501
Imipenem	Sigma-Aldrich	I0090000
Rifampicin	Sigma-Aldrich	557303
Valinomycin	Sigma-Aldrich	V0627
Vancomycin	Sigma-Aldrich	1709007
Polymyxin B	Sigma-Aldrich	81271
Gramicidin	Sigma-Aldrich	G0550000
Gemifloxacin	Sigma-Aldrich	SML1625
Colistin	Sigma-Aldrich	C4461
Ciprofloxacin	Sigma-Aldrich	17850
Luciferin-luciferase reagent	Yelen Analytics	Genofax A 500
L-glutamine	Invitrogen	25030081
Trypsin/EDTA Solution	Thermofischer Scientific	R001100
Resazurin Toxicity Kit	Sigma-Aldrich	TOX8
Puromycin	Sigma-Aldrich	P7255
Blasticidin	Sigma-Aldrich	203350
G418 Salt	Sigma-Aldrich	G8168
Experimental models: Cell lines		
Human kidney cell line model	American Type Culture Collection (ATCC)	A498 (ATCC HTB-44)
Human small intestinal cell line model	American Type Culture Collection (ATCC)	Caco-2 (ATCC HTB-37)
Human liver epithelial cell line model	American Type Culture Collection (ATCC)	HepG2 (ATCC HB-8065)
eLUCidate™ HeLa, TLR4/IL8 reporter cells	Genlantis	EL-TLR2293
Human erythrocyte	DivBioscience	–
Recombinant DNA		
pET-15b-*rumMc1-2*, two plasmids encoding the Radical-SAM enzymes RumMc1 and RumMc2, Ampicillin-resistant	Genscript	*rumMc1* GenBank: FQ670182.1, *rumMc2* GenBank: FQ670200.1
pETM-40-*rumC1-5*, five plasmids encoding the RumCs isoforms, Kanamycin-resistant	Genscript	*rumC1* Genbank: HM060266.1, *rumC2* Genbank: HM060267.1, *rumC3* Genbank: HM060268.1, *rumC4* Genbank: HM060269.1, *rumC5* Genbank: HM060270.1
psuf, encoding the suf machinery *sufABCDSE*, Chloramphenicol-resistant	Kind gift from Prof. Tadhg Begley, University of Texas	
Software and algorithms		
PyMol 2.5	https://pymol.org/2/	
Robetta	https://robetta.bakerlab.org	
APBS & PDB2PQR	https://www.poissonboltzmann.org/	

RESOURCE AVAILABILITY

Lead contact

Further information and requests for resources and reagents should be directed to and will be fulfilled by the Lead Contact, Mickael Lafond (michael.lafond@univ-amu.fr).

Materials availability

This study did not generate new unique reagents. All requests for resources should be directed to the lead contact author. All reagents will be made available on request after completion of a Materials Transfer Agreement.

Data and code availability

- This paper does not report original code.
- Any additional information required to reanalyze the data reported in this paper is available from the lead contact upon request.

EXPERIMENTAL MODEL AND SUBJECT DETAILS

Bacterial strains

Escherichia coli BL21(DE3) was used for the heterologous production of the five isoforms. The precultures were prepared in Luria-Bertani (LB) medium and incubated at 37°C overnight. Cultures were grown in M9 minimal medium containing kanamycin (50 μg/mL), ampicillin (100 μg/mL), chloramphenicol (34 μg/mL), vitamin B1 (0.5 μg/mL), $FeCl_3$ (50 μM), $MgSO_4$ (1 mM) and glucose (4 mg/mL) in a bioreactor (Inceltech LH.SGi, Discovery 100) of 12 L, at 37°C with moderate aeration (160 qnl/h) and 90 rpm agitation. Upon induction with IPTG, bacterial cultures were then incubated at 25°C.

Several bacterial strains were used for MICs determination and functional studies. Precultures of *Clostridium perfringens* ATCC 13124, *Clostridium difficile* DSMZ 1296 and *Helicobacter pylori* ATCC 43504 were prepared in BHI-YH medium and incubated overnight in a Trexler-type anaerobic chamber without stirring. On the other hand, the precultures of the oxygen-tolerant strains: *Listeria monocytogenes* DSM 20600, *Bacillus cereus* CIP 5257, *Bacillus subtilis* ATCC 6633, Vancomycin-resistant *Enterococcus faecalis* DSMZ 13591, Methicillin-resistant *Staphylococcus aureus* ATCC BAA-1717, *Vibrio alginolyticus* DSM 2172, *Escherichia coli* ATCC 8739, *Pseudomonas aeruginosa* ATCC 9027, *Acinetobacter baumanii* CIP 110431, and *Δ Escherichia coli (imp4213)* CIP 111272 were prepared in LB and incubated overnight at 37°C.

MICs determination was completed using MH medium with all bacterial strains except in the case of *C. perfringens* ATCC 13124, *C. difficile* DSMZ 1296 and *Streptococcus pneumoniae* R1501 where the MH medium was supplemented with 5% lysed horse blood and 20 mg/L β-nicotinamide adenine dinucleotide at 5.10^6 UCF/mL.

Cell lines

Three human cell lines were used in the cytotoxicity assays: A498 (ATCC HTB-44), Caco-2 (ATCC HTB-37) and HepG2 (ATCC HB-8065) being used as models of human kidney, small intestinal and liver epithelial cells, respectively. Cells were cultured in Dulbecco's modified essential medium (DMEM) supplemented with 10% fetal calf serum (FCS), 1% L-glutamine and 1% Streptomycin-Penicillin antibiotics (all from Invitrogen). Cells were routinely seeded and grown onto 25 cm^2 flasks maintained in a 5% CO_2 incubator at 37°C.

The commercial eLUCidate HeLa, TLR4/IL8 reporter cells (Genlantis) were routinely grown on 75 cm^2 flasks at 37°C with 5% CO_2 in DMEM supplemented with 10% FBS, 1% Pen/Strep and selection antimitotic agents, i.e., Puromycin (at 3 μg/mL), Blasticidin (at 5 μg/mL) and G418 (at 500 μg/mL) (all from Sigma-Aldrich).

METHOD DETAILS

Heterologous expression and purification of fully mature RumC1-5

pET-15b-*rumMc1-2* ampicillin resistant synthetic plasmids containing the *E. coli* codon-optimized gene of *R. gnavus* E1 encoding RumMc1 (GenBank: FQ670182.1) or RumMc2 (GenBank: FQ670200.1) were obtained from Genscript. pETM-40-*rumC1-5* kanamycin-resistant synthetic plasmids containing the *E. coli* codon-optimized gene of *R. gnavus* E1 encoding each RumC isoform (*rumC1* Genbank: HM060266.1, *rumC2* Genbank: HM060267.1, *rumC3* Genbank: HM060268.1, *rumC4* Genbank: HM060269.1, *rumC5* Genbank: HM060270.1), which allow the expression of MBP-tagged peptides, were obtained from Genscript. A TEV protease site is present in the linker between MBP tag and RumC1-5 peptides. Plasmids pET-15b-*rumMc1-2*, pETM-40-*rumC1-5* and *psuf* (chloramphenicol-resistant) containing *sufABCDSE* genes were used to transform competent *E. coli* BL21 (DE3) cells for expression. The resulting strain was grown in M9 medium containing kanamycin (50 μg/mL), ampicillin (100 μg/mL), chloramphenicol (34 μg/mL), vitamin B1 (0.5 μg/mL), $FeCl_3$ (50 μM), $MgSO_4$ (1 mM) and glucose (4 mg/mL). The culture was done in a bioreactor (Inceltech LH.SGi, Discovery 100) of 12 L, at 37°C with moderate aeration (160 qnl/h) and 90 rpm agitation. At an optical density (OD_{600}) of 0.6, $FeCl_3$ (50 μM) and L-cysteine (300 μM) were added and the culture was induced using 1 mM IPTG. The temperature was reduced to 25°C and the cells were grown for 15 h under stirring. Cells were then harvested by centrifugation (4,000 rpm for 20 min at 4°C). Cell pellet was resuspended in 150 mL of buffer A (50 mM Tris, pH 8, 50 mM NaCl) supplemented with three tablets of a protease inhibitor cocktail (cOmpleteTM, EDTA-free Protease inhibitor cocktail tablets, Roche). Cell pellet was then sonicated, and the lysate was clarified by centrifugation at 40,000 rpm for 30 min at 4°C. The supernatant was collected and passed over a Dextrin Sepharose High Performance column equilibrated with buffer A coupled to an FPLC (ÄKTA Pure 25, Cytiva). MBP-RumC1-5 were eluted with buffer B (50 mM Tris, pH 8, 50 mM NaCl, 40 mM Maltose). Fractions containing MBP-RumC1-5 were pooled and concentrated in a 10,000 MWCO Amicon Ultra centrifugal filter device. The samples were digested by TEV protease with a final TEV:MBP-RumC1-5 ratio of 1:100 (w/w) for 30 min at room temperature. MBP-tag, TEV protease and RumC1-5 were separated by loading over a HiLoad 26/600 Superdex 75 prep grade column (Cytiva) equilibrated in buffer C (HEPES 50 mM, NaCl 100 mM, pH 7.5). The peptide concentrations were estimated by UV-visible spectroscopy on

a Cary 50 UV-Vis Spectrophotometer (Varian) by using an extinction coefficient at 280 nm of 8,480 M^{-1} cm^{-1} for RumC1, 2980 M^{-1} cm^{-1} for RumC2, RumC3 and RumC5 and 4470 M^{-1} cm^{-1} for RumC4. Mature RumC1-5 isoforms were treated with Trypsin (TPCK, Sigma) for 1 h at 37°C, at a w/w ratio of 50:1 for RumC1-5:trypsin, to remove the leader peptide. RumC1-5 mature peptides free of their leader peptide were then purified by using a C18 preparative column (Phenomenex, Kinetex, 5 μm, 100 Å; 250 × 10 mm). The column is equilibrated with buffer D (90% H_2O, 10% acetonitrile, 0.1% trifluoroacetic acid) and subjected to a gradient from 0% to 30% of buffer E (90% acetonitrile, 10% H_2O, 0.1% trifluoroacetic acid) in 40 min on a ÄKTA Pure 25.

Mutant productions

Synthetic pETM40 plasmids (kanamycin-resistant) containing the *E. coli* codon-optimized gene encoding RumC1-A12E, RumC1-V4K, RumC1-S8G, RumC1-A44K, RumC2-E12A single mutants, and RumC2-K4V/G8S/E12A/K44A quadruple mutant were obtained from Genscript. These plasmids were used for the heterologous expression and purification of mature RumC1-2 mutants as described for RumC1-5 isoforms.

Nano-LC-MS/MS analyses

Heterologous RumC purified peptides were generally injected at a concentration of 0.1 μM. Sample were diluted in 5% (v/v) acetonitrile and 0.1% (v/v) trifluoroacetic acid and analyzed by online nano-LC–MS/MS (NCS HPLC, Dionex, and Qexactive plus, Thermo Fisher Scientific). Peptides were sampled on a 300 μm × 5 mm PepMap C18 precolumn and separated on a 75 μm × 250 mm C18 column (PepMap, Dionex). The nano-LC method consisted of a 40 min gradient at a flow rate of 300 nL/min, and MS and MS/MS data were acquired using Xcalibur (Thermo Fisher Scientific). High Collision Dissociation (HCD) energy of 22 was used in a Parallel Reaction Monitoring (PRM) experiment to target the species of interest after previous LC/MS run using an HCD energy of 27 and a DDA experiment (Data Dependant Analysis).

MS data analyses

Considering our knowledge from the natural RumC isoforms; we compared the MS/MS data and checked whether or not we had similarity of MS/MS ion signatures. We knew from the first data that having thioether bounds induce specific high y/b ions at the positions of the AA coupled to the cysteine and a loss of H_2. To complete the identifications, raw MS/MS data were also processed automatically using Mascot Distiller software (version 2.5.1, Matrix Science) followed by Mascot (version 2.6) searches using the sequences of the different peptides of interest as database. None was chosen as enzyme and the precisions were set at 10 ppm for the peptide precursor and 20 mmu for the fragments. Dehydramino (A, E, N, R, K) were set as variable modifications. Freestyle (Thermo Scientific) was used for the display and the deconvolution of the spectra. All considered experimental masses are mono-isotopic and non-protonated masses.

Structure prediction

Structural homology models were generated with the Robetta protein structure prediction server by using Rosetta Comparative Modeling and Ab Initio Modeling,[24,25] on the basis of the 3D-structure of RumC1 (PDB: 6T33). The electrostatic surface potential of each RumC isoform was evaluated by using the APBS & PDB2PQR software suite for biomolecular electrostatics and solvation.[26] Structural models were built using the PyMOL Molecular Graphics System, Version 2.0 Schrödinger, LLC.[27]

Membrane permeability assay

An overnight culture of *C. perfringens* ATCC 13124 was diluted at 1:100 in BHI-YH and grown at 37°C under anaerobic conditions until OD_{600} reached 0.3. Cells were then pelleted for 5 min at 3,500 g before being resuspended in sterile Phosphate-Buffered Saline (PBS) in their original volume. Propidium iodide (Sigma-Aldrich) was then added to the suspension at a final concentration of 40 μM. One hundred microliters of this suspension were then transferred into a 96-well black plate (Greiner Bio-One) and treated with RumC1, RumC3, RumC4, RumC5 or nisin at 5× their MIC values. Water and CTAB diluted at 300 μM final concentration were used as negative and positive controls, respectively. After 10-, 30- and 60-min incubation at 37°C under anaerobic conditions, fluorescence was measured (excitation at 530 nm and emission at 617 nm) using a microplate reader (Synergy Mx, BioTek). Results were expressed as the percentage of total permeabilization obtained by treatment with CTAB. For the permeabilization assay with Sytox Green (Thermo Fisher Scientific), a *C. perfringens* culture was prepared and treated with RumC1 or nisin at 5× their MIC values as described above. After 15 min, cells were stained with Sytox Green at 0.5 μM. Then, cells were rinsed with Hanks'balanced salt solution +/+ (Gibco) and resuspended in Vectashield (Vector Laboratories, CliniSciences H-1000). Observations were lastly performed with a Leitz DMRB microscope (Leïca), equipped with a Leïca DFC 450C camera. Fluorescence per cell surface was calculated with the software Fiji on a mean of 200 cells per condition. Fluorescence per cell surface was statistically analyzed by Mann-Whitney-Wilcoxon using the software R. All experiments were done in independent triplicate.

Flow cytometry

An overnight culture of *C. perfringens* ATCC 13124 was diluted at 1:100 in BHI-YH and grown at 37°C under anaerobic conditions until OD_{600} reached 0.3. Cells were then treated with RumC1 at 5x its MIC value for 15 and 60 min or left untreated. Cells were pelleted at 3,000 g for 5 min at 4°C before being diluted in an appropriate volume of PBS and analyzed by flow cytometry on a Bio-Rad S3E cells sorter. The blue laser (488 nm, 100 mW) was used for forward (FSC) and side scatter (SSC). Samples were run in the low-pressure mode at about 10,000 particles/s. The density plots obtained (small angle scattering FSC versus wide angle scattering SSC signal) were first gated on the population

of cells, then filtered to remove the multiple events. Populations of 500,000 events were used. Measurements were carried on independent triplicates. Results were analyzed and plotted using FlowJO v10.6.

Antibiotics

Antibiotics stock solutions were prepared according to the manufacturer guidelines in sterile conditions and stored at −20°C. The following antibiotics were all purchased from Sigma-Aldrich: mupirocin, metronidazole, fosfomycin, nisin, ampicillin, tetracycline, novobiocin, amoxicillin, kanamycin, nalidixic acid, streptomycin, imipenem, rifampicin, chloramphenicol, valinomycin, vancomycin, polymyxin B, gramicidin, gemifloxacin, colistin, ciprofloxacin.

MIC determination

Strains tested were acquired from commercial collections (the American Type Culture Collection (ATCC); the *Collection de l'Institut Pasteur* (CIP); the Leibniz Institute DSMZ Collection (DSM and DSMZ)) or from a laboratory collection (Laboratoire de Microbiologie et Genetique Moleculaires - Center for Integrative Biology in Toulouse). The MIC were determined by broth microdilution by independent triplicates according to the EUCAST 2022 recommendations except for the Clostridia and *Streptococcus pneumoniae*.[28] Briefly, a bacterial suspension of Clostridia and *S. pneumoniae* were grown in anaerobic conditions (in a Trexler-type anaerobic chamber without stirring) and adjusted in MH broth supplemented with 5% lysed horse blood and 20 mg/L β-nicotinamide adenine dinucleotide at 5.10^6 UCF/mL. Ninety microliters of cell suspension were transferred in a sterile F-bottom polypropylene 96-well microplates. Thus, 10 μL of sterile RumC1-5 from 100 to 0.1 μM by 2-fold serial dilutions were added to the bacterial suspension to obtain a final concentration of 5.10^5 CFU/mL. Microplates were incubated 48 h at 37°C in anaerobic conditions. MIC was defined as the lowest concentration of peptide that inhibited the growth of bacteria after 48 h incubation at 37°C. Sterility and growth controls were prepared for each assay. All experiments were done in independent triplicates.

ATP bioluminescent assays

C. perfringens ATCC 13124 was grown in BHI-YH broth in anaerobic conditions (in a Trexler-type anaerobic chamber without stirring) at 37°C until OD_{600} nm reached 0.35. Then *C. perfringens* cells were distributed in white polystyrene Nunc 96-well plate (ThermoFisher Scientific) and RumC1, RumC3, RumC4, RumC5 or nisin were added at 2.5, 5 or 10 x MIC. After 15 min incubation in the same conditions, 100 μL of cells were mixed with 10 μL of luciferin-luciferase reagent (Yelen Analytics) prepared in IMI-Yelen Buffer (Yelen Analytics). The mix was homogenized and incubated 30 s before reading of the emitted photon using a microplate reader (Synergy Mx, BioTek). Then, 10 μL of lysis reagent (Yelen Analytics) was added to the mixture, homogenized and incubated 1 min before a new reading of the emitted photon. The intensity of the bioluminescent light was expressed as relative light units (RLU) which is proportional to extracellular ATP concentration.[29] The inner ATP concentration was derived from the difference in ATP concentration in the extracellular media before and after cell lysis. Results were expressed as a percentage of total inner ATP signal that was measured with untreated cells. All experiments were done in triplicates.

Minimal equimolar inhibitory concentration (MEIC) determination

MIEC were determined using the same protocol as MIC determination with the following modifications. Instead of starting the 2-fold serial dilutions with 100 μM of one RumC isoform, combination of two isoforms were added to obtain a equimolar concentration of 25 μM for each isoform before performing the serial dilutions. The MIEC was defined as the lowest concentration at which no bacterial growth is detected after incubation and as the addition of each isoform concentration present in that well. A ratio (lowest MIC of the pair)/MIEC ratio ≥ 1 suggests an additive or synergic effect whereas a ratio ≤ 0.5 indicate a neutral or antagonist effect. Once an additive or synergic combination was detected, it was further analyzed using the checkboard assay. All experiments were done in independent duplicates.

Checkerboard assay

The first compound of the combination to be assayed was added to all the wells of the first row to obtain a final concentration corresponding to twice the previously obtained MIC value and in a total volume of 100 μL. Then, 2-fold serial dilutions in culture medium were done from one row to another using 50 μL. Similarly, the second compound was added into the wells of the last column and 2-fold serial dilutions were done this time from one column to another. Then, 100 μL of bacterial suspensions (prepared as described for MIC determination) were added to each well to obtain a final volume of 150 μL per well. For each compound, dilution were not performed in the last row or column to measure the effect of each compound alone as well. Plates were incubated as described above. All the wells where no growth was detected after incubation were used to calculate the fractional inhibitory concentration index (FICi) as follows:

$$FICi = (C_1 / MIC_1) + (C_2 / MIC_2)$$

C1 = Concentration of the first compound in the wellMIC1 = MIC value of the first compound when used aloneC2 = Concentration of the second compound in the wellMIC2 = MIC value of the second compound when used alone

If one of FICi values is less than or equal to 0.5, it indicates a synergy. If all values of FICi are between 0.5 and 4, they indicate a neutral or an additive effect. Lastly, a value greater than 4 indicates an antagonistic affect. An example of Checkerboard assay and FICi calculation is presented on Table S1. Sterility and growth controls were prepared for each assay and all experiments were done in independent duplicates.

Time-kill kinetics assay

C. perfringens ATCC 13124 was grown in BHI-YH in anaerobic conditions at 37°C overnight. For the studies on log phase cells, the overnight culture was diluted to 1:100 in BHI-YH and grown until OD_{600} reached 0.3 before being treated with RumC1, nisin, vancomycin, or metronidazole at 5xMIC. For the studies on stationary phase cells, the overnight culture was treated directly with the same antimicrobials at 5 or 10xMIC. In both cases, untreated cells were used as a control of natural growth and death. Cells were incubated in anaerobic conditions. At 15, 30 min, 1, 2, 4, 6, 24, 48 h, 20 μL of each cell suspension were collected and serial diluted. Dilutions were plated on BHI-YH agar and after 24 h of growth in anaerobic conditions at 37°C, colonies were counted to determine the CFU/mL. For the log phase studies, each condition was repeated twice independently. For the stationary phase studies, each antimicrobial was studied once at the two concentrations.

Hemolytic activity assay

The hemolytic activity of RumC1-5 was evaluated as previously described.[30–32] Briefly, human erythrocytes (obtained from Divbioscience, NL) were pelleted by centrifugation at 800 *g* for 5 min. Cell pellet was then resuspended in sterile PBS and centrifuged at 800 g for 5 min. This step was repeated three times and erythrocytes were finally resuspended in Dulbecco's modified essential medium (DMEM, Invitrogen) supplemented with 10% fetal calf serum (FCS, Invitrogen) at a concentration of 8%. One hundred μL were then added per well of sterile 96 well microplates (Greiner) containing 100 μL of DMEM +10% FCS with increasing concentrations of RumC1-5 (from 0 to 100 μM) obtained by 2-fold serial dilutions. Sterile water and Triton X-100 diluted in media at 0.1% (v/v) were used as negative and positive controls, respectively. After 1 h at 37°C, the microplates were centrifuged at 800 g for 5 min. One hundred μL of cell supernatants were collected and transferred to a new 96 well microplates and OD405 nm was measured using microplate reader (Synergy Mx, Biotek). Hemolysis caused by RumC1-5 was expressed as percentage of total hemolysis given by treatment with Triton X-100 at 0.1%. All experiments were done in triplicate.

Cytotoxic activity assay

The toxicity of RumC1-5 as well as a combination of RumC1 with amoxicillin (Sigma-Aldrich) at a molar ratio 1:1 was evaluated on human cell lines: A498 (ATCC HTB-44), Caco-2 (ATCC HTB-37) and HepG2 (ATCC HB-8065) being used as models of human kidney, small intestinal and liver epithelial cells, respectively. Cells were cultured in Dulbecco's modified essential medium (DMEM) supplemented with 10% fetal calf serum (FCS), 1% L-glutamine and 1% Streptomycin-Penicillin antibiotics (all from Invitrogen). Cells were routinely seeded and grown onto 25 cm^2 flasks maintained in a 5% CO_2 incubator at 37°C. Prior to cytotoxicity assay, cells grown on 25 cm^2 flasks were detached using trypsin–EDTA solution (from Thermo Fisher Scientific), counted using Mallasez counting chamber and seeded into 96-well cell culture plates (Greiner bio-one) at approximately 10^4 cells per well. The cells were left to reach confluence for 48–72 h at 37°C in a 5% CO_2 incubator. Plates were then aspirated and increasing concentrations of RumC1-5 diluted in culture medium were added to the cells for 48 h at 37°C in a 5% CO_2 incubator. Sterile water was used as negative control. At the end of the incubation, wells were empty and cell viability was evaluated using resazurin-based *in vitro* toxicity assay kit (from Sigma-Aldrich) following manufacturer's instructions.[33] Briefly, wells were aspirated and were filled with 100 μL of diluted resazurin solution obtained by dilution of the resazurin stock solution 1:100 in sterile PBS containing calcium and magnesium (PBS++, pH 7.4, from Thermo Fisher Scientific). After 4 h incubation at 37°C, fluorescence intensity was measured using microplate reader (Synergy Mx, Biotek) with an excitation wavelength of 530 nm and an emission wavelength of 590 nm. The fluorescence values were normalized by the control and expressed as percentage of cell viability. All experiments were done in triplicate.

Anti-inflammatory activity

Anti-inflammatory activity of RumC1-5 as well as a combination of RumC1 with amoxicillin (Sigma-Aldrich) at a molar ratio 1:1 was evaluated using the commercial eLUCidate HeLa, TLR4/IL8 reporter cells (Genlantis) and as previously described.[19] This reporter cell line corresponds to a stably transfected HeLa cells which express human TLR4 as well as Renilla luciferase reporter gene under the transcriptional control of the IL-8 promoter, making them a valuable model to detect activation of IL-8 expression by stimuli causing NFkB activation such as IL-1. Cells are routinely grown on 75 cm^2 flasks at 37°C with 5% CO_2 in DMEM supplemented with 10% FBS, 1% Pen/Strep and selection antimitotic agents, i.e., Puromycin (at 3 μg/mL), Blasticidin (at 5 μg/mL) and G418 (at 500 μg/mL) (all from Sigma-Aldrich). To evaluate the anti-inflammatory effect of RumC1-5, eLUCidate HeLa cells were detached from 75 cm^2 flasks using Trypsin-EDTA solution (Thermo-Fisher), counted using Malassez counting chamber and seeded into 96-well cell culture plates (Greiner bio-one) at approximately 50,000 cells per well following manufacturer's instructions. The next day, wells were emptied and cells were left untreated (negative controls) or were treated with 100 μL of culture medium containing 10 ng/mL of human recombinant IL-1 beta (Peprotech) in the presence of increasing concentrations of RumC1-5 (from 0 to 100 μM, serial 1:2 dilutions). Importantly, all steps were performed using non-pyrogenic plastics and RNase/DNase molecular biology tips to limit the risk of presence of trace of LPS. After 6 h incubation at 37°C with 5% CO_2, wells were emptied and the cells were lysed during 10 min at 4°C with 70 μL of ice-cold PBS containing 1% Triton X-100. Fifty μL of cell lysates were then transferred into white 96-well luminescence plates (Dominique Dutscher) already containing 100 μL of Renilla luciferase substrate (Yelen). Luminescence signals of the wells were immediately measured using microplate reader (Biotek, Synergy Mx). All experiments were done in triplicate.

QUANTIFICATION AND STATISTICAL ANALYSIS

The MICs presented in Tables 1 and 2 are the average of values obtained from independent triplicates.

The quantitative data displayed in Figures 2 and 3 are presented as the mean ± standard deviation (SD) of independent triplicates.

The fluorescent signal per cell surface in the membrane permeabilization assays was quantified on a mean of 200 cells from different fields and statistically analyzed by Mann-Whitney-Wilcoxon test using the R software. p values are indicated on the Figure S3. The results presented were obtained from independent triplicates.

Flow cytometry density plots presented in Figure S3 (small angle scattering FSC versus wide angle scattering SSC signal) were first gated on the population of cells, then filtered to remove the multiple events. Populations of 500,000 events were used. Measurements were carried on independent triplicates. Results were analyzed and plotted using FlowJO v10.6. The results were obtained from independent triplicates.